



Freiburg Neuropathology Case Conference

A 43-year-old Patient Presenting with a Right-sided, Slowly Progressing, Painless Exophthalmos and Ptosis

B. Simon^{1,4} · E. Wogram^{2,4} · A. T. Camp^{3,4} · M. Prinz^{2,4} · H. Urbach^{1,4} · D. Erny^{2,4} · C. A. Taschner^{1,4}

Accepted: 24 January 2023 / Published online: 20 February 2023
© The Author(s) 2023

Keywords Primary orbital lymphoma · Orbital metastasis · Orbital rhabdomyosarcoma · Orbital schwannoma · Orbital solitary fibrous tumor

Case Report

A 43-year-old male patient presented with a painless 5 mm exophthalmos of the right eye (OD), which had slowly developed over the past 12 months concurrently with a right-sided ptosis. He did not report any double vision.

On examination the palpebral aperture measured 5 mm OD and 10 mm for the left eye (OS). There was no swelling, redness or hyperthermia of the right eyelid. Ocular motility OD was largely unremarkable except for a slight elevation and abduction deficit on wide gaze excursion. Best-corrected visual acuity (BCVA) was 20/25 Snellen (0.8 dec) OD and 25/25 Snellen (1.0 dec) OS. Ophthalmological examination showed no evidence of optic nerve compression OD with no relative afferent pupillary defect, inconspicuous funduscopy and optical coherence tomography of the retina and peripapillary retinal nerve fiber layer.

A transnasal biopsy of the tumor previously performed at a peripheral hospital had shown unspecific results.

The multidisciplinary tumor board recommended surgical excision of the tumor. Surgery was performed via a transconjunctival approach in general anesthesia using a surgical microscope as described previously [1]. Oculopression was performed preoperatively to lower eye pressure, facilitate lateral displacement of the globe within the orbit and thereby widen the surgical corridor. The conjunctiva was incised over 270° in the medial circumference. The superior and inferior rectus muscles were tethered with 4-0 silk retraction sutures. The medial rectus muscle was detached from the globe. Another 4-0 silk retraction suture at the muscle's insertion point was used to displace the globe laterally. Into the medial quadrant of the parabolbar space, two narrow spatulas and one wide orbital spatula (Fig. 1) were inserted to form a triangular viewing channel. Spatula blades were inserted flat sides together and rotated into an orthogonal position once in place, thereby carefully displacing orbital structures sideways. In the depth of the parabolbar space, orbital fat was found. Its fine septa were opened with scissors at the tumor's suspected location, revealing a homogeneous, white-colored, smoothly encapsulated tumor abutting the medial rectus muscle. A primary docking attempt with a cryostat was insufficient, so tumor grasping forceps were used for removal. Macroscopically, the tumor was a homogeneous, whitish, encapsulated, clearly circumscribed mass. Close microscopic inspection of the tumor bed confirmed complete removal and sufficient hemostasis after coagulation. The patient reported no pain or double vision 1 day after surgery. The BCVA OD was 20/50 Snellen (0.4 dec), likely due to swelling and irritation of the conjunctiva. No clinical signs of optic nerve compression were

The authors B. Simon and E. Wogram contributed equally to the manuscript.

✉ C. A. Taschner
christian.taschner@uniklinik-freiburg.de

- 1 Department of Neuroradiology, University of Freiburg, Freiburg, Germany
- 2 Department of Neuropathology, University of Freiburg, Freiburg, Germany
- 3 Department of Ophthalmology, University of Freiburg, Freiburg, Germany
- 4 Medical Centre—University of Freiburg, Faculty of Medicine, University of Freiburg, Breisacherstr. 64, 79106 Freiburg, Germany

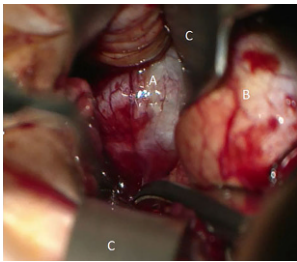


Fig. 1 View of the operative site: tumor (A), right eyeball (B), spatulas (C)

observed. After 2 days the patient was discharged from the hospital.

Imaging

Magnetic resonance (MR) imaging showed an intraorbital, intraconal space-occupying lesion located medially of the right optic nerve (Figs. 2 and 3, arrows). T2-weighted images (Fig. 2a, b, arrows) showed cystic components. Note the right-sided exophthalmos on axial images (Figs. 2a and 3a, b). On T1-weighted images the lesion appeared isointense (Fig. 3a, arrow). After administration of gadolinium (Gd) the lesion displayed distinct and homogeneous contrast enhancement (Fig. 3b, c, arrows). On diffusion-weighted images (B1000) the lesion showed no signs of restricted diffusion (not shown).

Differential Diagnosis

Orbital Lymphoma

Primary lymphoma of the orbit is a B-cell non-Hodgkin lymphoma and one of the most common orbital tumors,

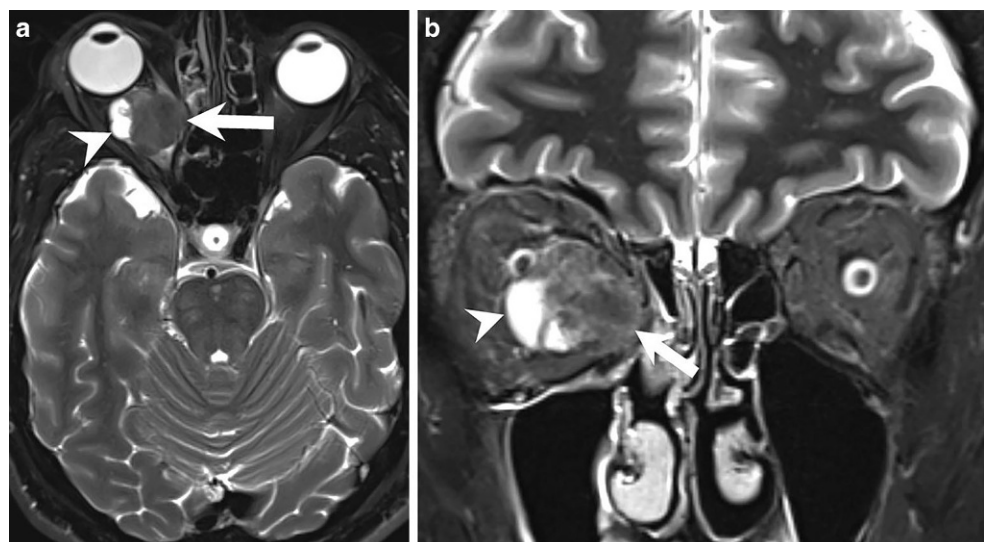
accounting for as much as half of all orbital malignancies. On imaging, orbital lymphoma usually appear as a soft tissue mass, often located in the upper outer quadrant in association with the lacrimal gland [2]. In distinguishing lymphomas from other orbital tumors, the extraocular muscles can be encircled or displaced. However, extraocular muscles are usually not the origin of the mass lesion. Infiltration of the optic nerve or eyeball is also rare. Similar to intracranial lymphomas they are homogeneous in density with high cellularity resulting in restricted diffusion on diffusion-weighted imaging (DWI), isointensity to hypointensity compared to muscle in T1-weighted sequences and isointense to hyperintense signal compared to muscle in T2-weighted imaging. After administration of Gd they show homogeneous enhancement [3, 4].

Orbital lymphoma seemed a valid differential diagnosis as the imaging criteria matched and lymphomas account for a large proportion of malignant orbital masses.

Metastases

Orbital metastases are relatively uncommon with breast cancer being the most common malignancy to metastasize to the orbit, followed by prostate cancer, melanoma, and lung cancer [5]. Extraocular orbital metastases are usually unilateral and only rarely primarily involve the extraocular muscles, although secondary involvement may commonly occur [6]. Thyroid and prostate metastases can be located in the bony margins of the orbit. Radiographic features are variable both in computed tomography (CT) and MR imaging. The morphology ranges from well-defined to diffusely infiltrating lesions. Usually contrast enhancement is present but can be very variable. Bony destruction may be present. MR imaging shows its superiority compared to CT in greater contrast resolution making it invaluable in the as-

Fig. 2 Axial (a) and coronal (b) T2-weighted images showed an intraorbital, intraconal mass (arrows) located medially of the optic nerve. Cystic components were presented on the lateral tumor margin (arrowheads). Note the right-sided exophthalmos on the axial view (a)



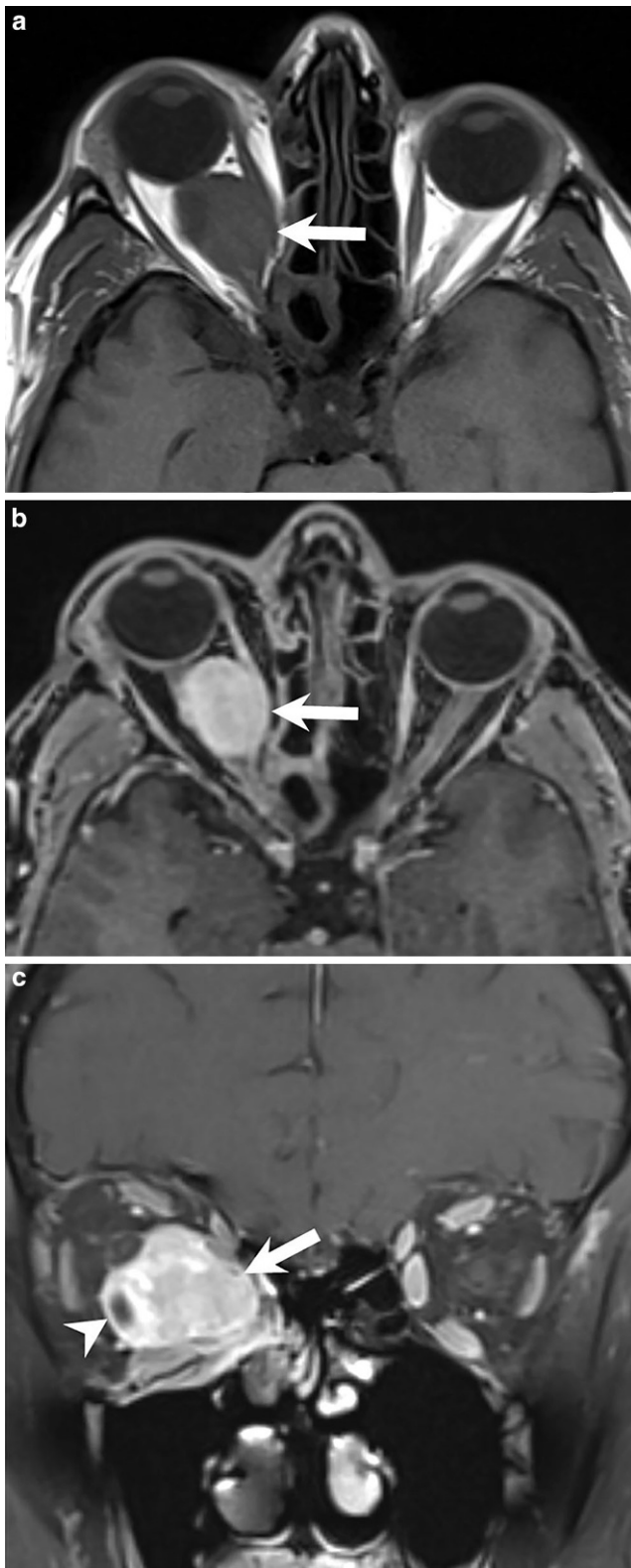


Fig. 3 On T1-weighted axial images (a) without contrast the lesion (arrow) appeared isointense. On axial (b) and coronal (c) T1-weighted images MRI after administration of Gd the lesion showed homogeneous enhancement of contrast (arrows). The cystic portion of the tumor displayed a contrast-enhancing capsule (c, arrowhead)

assessment of orbital masses. Fat-suppression techniques and post-contrast T1-weighted images with thin slices and a reduced field of view are paramount for initial assessment [5, 7].

Although relatively uncommon in the orbit, metastases should always be considered as a differential diagnosis.

Orbital Rhabdomyosarcoma

Rhabdomyosarcoma (RMS) is a highly malignant tumor. It has been reported from birth up to the seventh decade of life, with the majority of cases presenting in early childhood making it the most common soft tissue sarcoma of the head and neck in childhood. Orbital RMS is usually located extraconally or extending both intraconally and extraconally with close proximity to extraocular muscles. In early stages the tumor is usually well circumscribed, whereas in later stages borders become irregular [8]. On imaging, RMS are typically homogeneous soft tissue masses isodense to muscle and may show extension into the eyelid or through bony structures. MRI is the modality of choice for evaluating soft tissue tumors and plays an important role in initial diagnosis and assessment of tumor response after treatment [9]. RMS appear with low to intermediate intensity and isointense signal to adjacent muscles in T1-weighted sequences. They generally show vivid contrast enhancement. Because of high cellular density RMS usually have restricted diffusion on DWI [10, 11]. In terms of imaging features and tumor growth we considered RMS to be a possible diagnosis.

Orbital Schwannoma

Schwannomas are benign nerve sheath tumors that originate from the Schwann cells of the perineurium of peripheral nerves. They are the most common benign peripheral nerve tumors in adults but rarely occur in the orbit [12]. Orbital schwannomas account for only 1% of all orbital tumors and commonly arise from supraorbital and supratrochlear nerves in the upper anterior orbital cavity [12, 13].

It is difficult to differentiate orbital schwannomas from other intraorbital tumors. They are homogeneous, elongated, and oval to spindle-shaped lesions with a density similar to extraocular muscles. General imaging features include cystic and fatty degeneration. In larger schwannomas cystic degeneration or hemorrhage may occur and calcifications are rare. CT has less diagnostic value but may show characteristic expansion into bone. On MR imaging, orbital schwannomas are usually hypointense in T1-weighted imaging and hyperintense on T2-weighted imaging. After administration of Gd schwannomas enhance, either homogeneously or heterogeneously [14, 15]. In our case, we considered orbital schwannoma a valid differential diagnosis

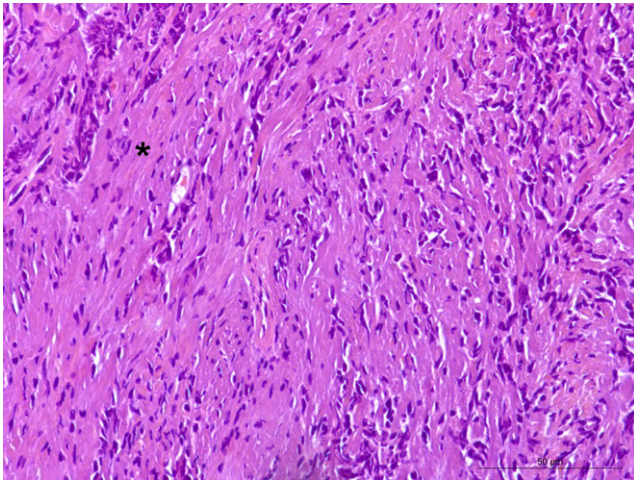


Fig. 4 Hematoxylin-eosin-stained section depicted an isomorphic tumor formation with spindle-shaped cells and a streaming of tumor cells between collagen. Asterisk indicates collagenous stroma. Scale bar: 50 μ m

based on its location and cystic and solid appearance with vivid Gd enhancement.

Solitary Fibrous Tumor

Solitary fibrous tumors (SFT) are rare mesenchymal neoplasms which account for less than 2% of all soft tissue tumors [16]. They usually present as a solitary well-circumscribed mass located in intraconal and extraconal spaces of the orbit. The lesion may show calcifications and necrosis with high vascularization. Also remodeling of the adjacent bone may be seen in larger tumors [17]. Isointense to hypointense signal on T2-weighted images and vivid enhancement with probable washout pattern are the main MRI characteristics of orbital SFT. Internal hemorrhage, cysts or fibrosis are best demonstrated in T2-weighted sequences as well [18, 19]. Although a rare entity, if imaging criteria are

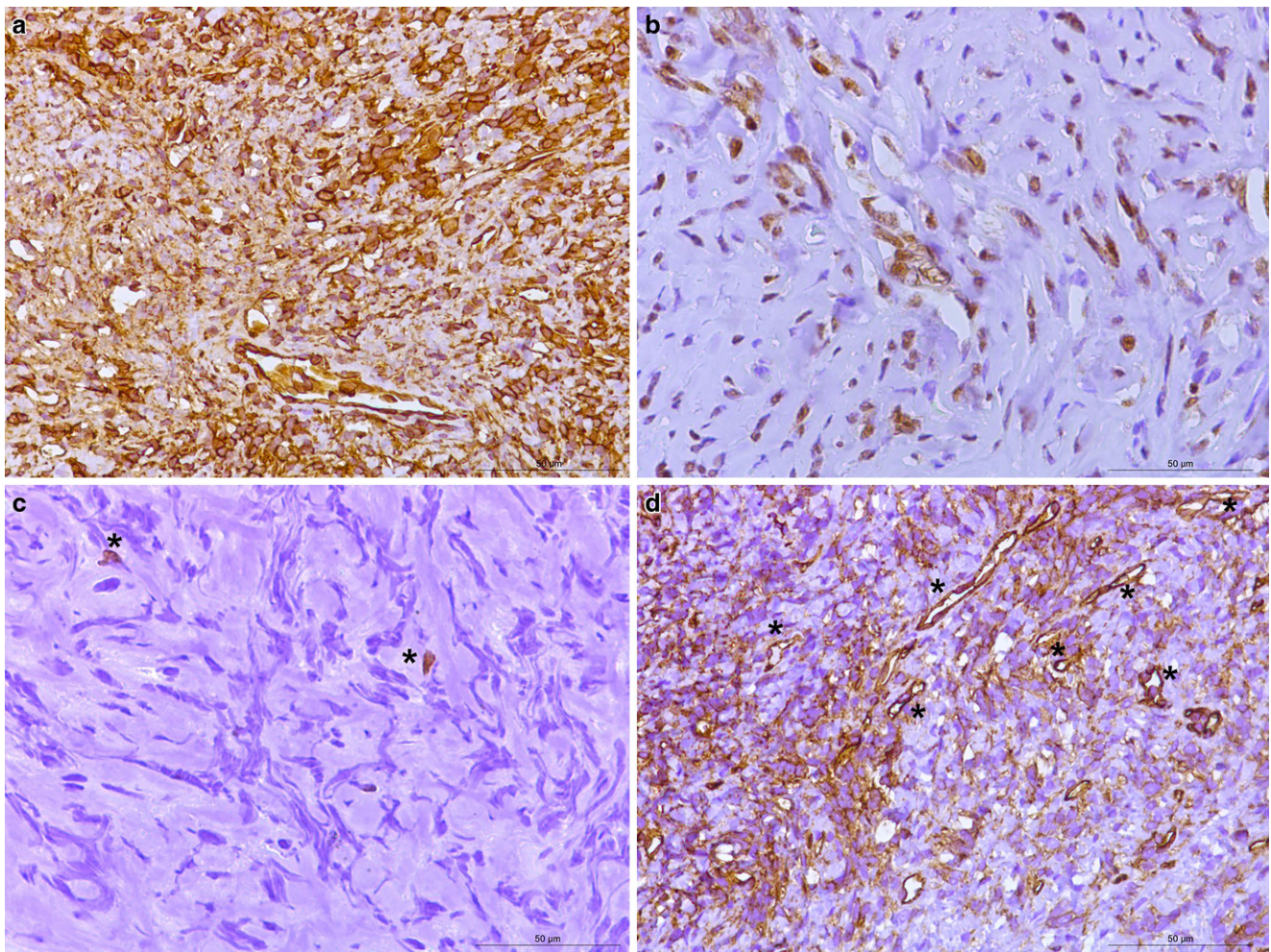


Fig. 5 Immunohistochemistry: homogeneously positive reaction in the tumor cells for vimentin (a). Tumor cells showed a positive reaction for STAT6 (b). Immunohistochemistry for Ki-67 (Mib1), detected about 1% of all the tumor cells that were proliferating (c) with asterisks indicating two proliferating cells. Immunohistochemistry for CD34 (d) showed a positive reaction in the endothelial cells that constituted the dilated, branched, hyalinized staghorn-like (hemangiopericytoma-like) vasculature. Asterisks indicate a few exemplary vessels. Scale bars: 50 μ m

met SFT may be included in the differential diagnosis of orbital soft tissue masses.

Histology and Immunohistochemistry

In the hematoxylin-eosin (H&E) stained section of the formaldehyde-fixed and paraffin-embedded biopsy material, an isomorphic tumor was detected with moderately increased cellularity (Fig. 4). The tumor cells were mostly isomorphic and spindle-shaped. An increased number of blood vessels, and a collagenous stroma with streaming of cells between collagen was observed. No mitotic figures were identified. Fresh hemorrhages were present in a few, small regions. No traces of old hemorrhages were identified with the Prussian blue reaction (not shown). The tumor cells reacted positively in the immunohistochemistry for vimentin (Fig. 5a). In the immunohistochemistry for signal transducer and activator of transcription 6 (STAT6), a strong positive signal was observed in the nuclei of the tumor cells (Fig. 5b). The immunohistochemistry for inhibin, S100, pan-cytokeratin (PanCK), epithelial membrane antigen (EMA), and glucose transporter 1 (GLUT1) were negative in the tumor cells (not shown). The reaction for Ki-67 (Mib1) marked about 1% of all the tumor cells (Fig. 5c, asterisks). Numerous blood vessels (less so in number and intensity the tumor cells) were marked by the immunohistochemistry for CD34 (Fig. 5d, asterisk) and Wilm's tumor protein (WT1, not shown). The positive immunohistochemistry for CD34 is characteristic (albeit nonspecific) for solitary fibrous tumors (SFT), especially low-grade SFT. The positive reaction for STAT6 in the tumor nuclei constitutes a very highly sensitive and specific marker for SFT [20]. About 98% of SFT cases have been described to show nuclear expression of STAT6, making it the most specific immunohistochemical marker [21]. Nuclei positivity for STAT6 thereby reliably differentiates SFTs from meningioma, meningeal Ewing's sarcoma, mesenchymal chondrosarcoma, malignant peripheral nerve sheath tumor, and synovial sarcomas [20]. To further rule out the differential diagnosis of a malignant peripheral nerve sheath tumor, immunohistochemistry for S100 was performed, which produced a negative result (not shown). Likewise, immunohistochemistry was used to check for the presence of monophasic synovial sarcomas, again, yielding a negative result (not shown). The nuclei in this sample were oval but lacked the pseudoinclusions typical for meningioma. In addition, no calcifications or psammoma bodies were observed. Both observations ruling out the presence of a meningothelial neoplasm.

Diagnosis

Solitary fibrous tumor (SFT) of the orbit

Solitary fibrous tumors are rare mesenchymal tumors that arise at a plethora of anatomic sites, especially in deep soft tissues, and particularly in the thigh, pelvic fossa, retroperitoneum, and serosal surfaces [22–24]. The tumor cells carry a NAB2:STAT6 gene fusion, which is a result of a paracentric inversion involving chromosome 12q13 [20]. Orbital SFT appear mostly in middle-aged patients and are predominantly located in the superior aspect of the orbit [25]. Previous reports have concluded that orbital SFT are mostly benign tumors with a low recurrence rate of approximately 16% [26–29]. Surgical excision is the treatment of choice but can be difficult to achieve [25]. Head and neck solitary fibrous tumors demonstrate a significantly larger local recurrence rate as compared with the rate of metastasis. They can recur many years after initial treatment, warranting long-term surveillance and follow-up to assess for tumor recurrence [30]. Malignant SFT is extremely rare and it can be difficult to distinguish between benign and malignant SFT. Generally, malignant SFTs are larger than benign SFTs and common gross features are hemorrhage and/or necrosis in the malignant neoplasm [31]. Recent studies suggest that the presence of a telomerase reverse transcriptase (TERT) promoter mutation resulting in its overexpression may be associated with a shorter disease-free survival [32, 33].

Funding Open Access funding enabled and organized by Projekt DEAL.

Declarations

Conflict of interest B. Simon, E. Wogram, A.T. Camp, M. Prinz, H. Urbach, D. Erny and C.A. Taschner declare that they have no competing interests.

Ethical standards All investigations described in this manuscript were carried out with the approval of the responsible ethics committee and in accordance with national law and the Helsinki Declaration of 1975 (in its current revised form). Informed consent was obtained from the patient in this case if identifiable from pictures or other information within the manuscript.

Open Access This article is licensed under a Creative Commons Attribution 4.0 International License, which permits use, sharing, adaptation, distribution and reproduction in any medium or format, as long as you give appropriate credit to the original author(s) and the source, provide a link to the Creative Commons licence, and indicate if changes were made. The images or other third party material in this article are included in the article's Creative Commons licence, unless indicated otherwise in a credit line to the material. If material is not included in the article's Creative Commons licence and your intended use is not permitted by statutory regulation or exceeds the permitted use, you will need to obtain permission directly from the copyright holder. To view

a copy of this licence, visit <http://creativecommons.org/licenses/by/4.0/>.

References

- Lagrèze WA, Augustynik M, Biermann J, Gross N. Technik und Ergebnisse der transkonjunktivalen Entfernung orbitaler Hämangiome [Technique and Results for the Transconjunctival Removal of Orbital Haemangiomas]. *Klin Monbl Augenheilkd*. 2016;233:24–8. Erratum in: *Klin Monbl Augenheilkd*. 2016;233:e1.
- Ferreri AJ, Dolcetti R, Du MQ, Doglioni C, Resti AG, Politi LS, De Conciliis C, Radford J, Bertoni F, Zucca E, Cavalli F, Ponzoni M. Ocular adnexal MALT lymphoma: an intriguing model for antigen-driven lymphomagenesis and microbial-targeted therapy. *Ann Oncol*. 2008;19:835–46. <https://doi.org/10.1093/annonc/mdm513>.
- Maksimovic O, Bethge WA, Pintoff JP, Vogel M, Claussen CD, Bares R, Horger M. Marginal zone B-cell non-Hodgkin's lymphoma of mucosa-associated lymphoid tissue type: imaging findings. *AJR Am J Roentgenol*. 2008;191:921–30. <https://doi.org/10.2214/AJR.07.2629>.
- Priego G, Majos C, Climent F, Muntane A. Orbital lymphoma: imaging features and differential diagnosis. *Insights Imaging*. 2012;3:337–44. <https://doi.org/10.1007/s13244-012-0156-1>.
- Taylor TD, Gupta D, Dalley RW, Keene CD, Anzai Y. Orbital neoplasms in adults: clinical, radiologic, and pathologic review. *Radiographics*. 2013;33:1739–58. <https://doi.org/10.1148/rg.336135502>.
- Char DH, Miller T, Kroll S. Orbital metastases: diagnosis and course. *Br J Ophthalmol*. 1997;81:386–90. <https://doi.org/10.1136/bjo.81.5.386>.
- Meltzer DE. Orbital imaging: a pattern-based approach. *Radiol Clin North Am*. 2015;53:37–80. <https://doi.org/10.1016/j.rcl.2014.09.004>.
- Jurdy L, Merks JH, Pieters BR, Mourits MP, Kloos RJ, Strackee SD, Saeed P. Orbital rhabdomyosarcomas: a review. *Saudi J Ophthalmol*. 2013;27:167–75. <https://doi.org/10.1016/j.sjopt.2013.06.004>.
- Inarejos Clemente EJ, Navallas M, Barber Martínez de la Torre I, Suñol M, Munuera Del Cerro J, Torner F, Garraus M, Navarro OM. MRI of rhabdomyosarcoma and other soft-tissue sarcomas in children. *Radiographics*. 2020;40:791–814. <https://doi.org/10.1148/rg.2020190119>.
- Karcioglu ZA, Hadjistilianou D, Rozans M, DeFrancesco S. Orbital rhabdomyosarcoma. *Cancer Control*. 2004;11:328–33. <https://doi.org/10.1177/107327480401100507>.
- Jurdy L, Merks JH, Pieters BR, Mourits MP, Kloos RJ, Strackee SD, Saeed P. Orbital rhabdomyosarcomas: a review. *Saudi J Ophthalmol*. 2013;27:167–75. <https://doi.org/10.1016/j.sjopt.2013.06.004>.
- Chaskes MB, Rabinowitz MR. Orbital Schwannoma. *J Neurol Surg B Skull Base*. 2020;81:376–80. <https://doi.org/10.1055/s-0040-1713935>.
- Chen MH, Yan JH. Imaging characteristics and surgical management of orbital neurilemmomas. *Int J Ophthalmol*. 2019;12:1108–15. <https://doi.org/10.18240/ijo.2019.07.09>.
- Beaman FD, Kransdorf MJ, Menke DM. Schwannoma: radiologic-pathologic correlation. *Radiographics*. 2004;24:1477–81. <https://doi.org/10.1148/rg.245045001>.
- Skolnik AD, Loevner LA, Sampathu DM, Newman JG, Lee JY, Bagley LJ, Learned KO. Cranial nerve Schwannomas: diagnostic imaging approach. *Radiographics*. 2016;36:1463–77. <https://doi.org/10.1148/rg.2016150199>.
- Tariq MU, Din NU, Abdul-Ghafar J, Park YK. The many faces of solitary fibrous tumor; diversity of histological features, differential diagnosis and role of molecular studies and surrogate markers in avoiding misdiagnosis and predicting the behavior. *Diagn Pathol*. 2021;16:32. <https://doi.org/10.1186/s13000-021-01095-2>.
- Kim HJ, Lee HK, Seo JJ, Kim HJ, Shin JH, Jeong AK, Lee JH, Cho KJ. MR imaging of solitary fibrous tumors in the head and neck. *Korean J Radiol*. 2005;6:136–42. <https://doi.org/10.3348/kjr.2005.6.3.136>.
- Yang BT, Wang YZ, Dong JY, Wang XY, Wang ZC. MRI study of solitary fibrous tumor in the orbit. *AJR Am J Roentgenol*. 2012;199:W506–11. <https://doi.org/10.2214/AJR.11.8477>.
- Kim HJ, Kim HJ, Kim YD, Yim YJ, Kim ST, Jeon P, Kim KH, Byun HS, Song HJ. Solitary fibrous tumor of the orbit: CT and MR imaging findings. *AJNR Am J Neuroradiol*. 2008;29:857–62. <https://doi.org/10.3174/ajnr.A0961>.
- Louis DN, Aldape KD, Capper D, Giannini C, Horbinski CM, Ng HK, Board WCo. Glioblastoma, IDH-wildtype. In: WHO Classification of Tumours Editorial Board, editor. WHO classification of tumours 5th edition central nervous system tumours. 5th ed. Lyon: International Agency for Research on Cancer; 2021.
- Doyle LA, Vivero M, Fletcher CD, Mertens F, Hornick JL. Nuclear expression of STAT6 distinguishes solitary fibrous tumor from histologic mimics. *Mod Pathol*. 2014;27:390–5.
- Gold JS, Antonescu CR, Hajdu C, Ferrone CR, Hussain M, Lewis JJ, Brennan MF, Coit DG. Clinicopathologic correlates of solitary fibrous tumors. *Cancer*. 2002;94:1057–68.
- Gupta S, Verma R, Sen R, Singh I, Marwah N, Kohli R. Solitary fibrous tumor of the orbit. *Asian J Neurosurg*. 2016;11:78. <https://doi.org/10.4103/1793-5482.165804>.
- McMaster MJ, Soule EH, Ivins JC. Hemangiopericytoma. A clinicopathologic study and long-term followup of 60 patients. *Cancer*. 1975;36:2232–44.
- Ali MJ, Honavar SG, Naik MN, Vemuganti GK. Orbital solitary fibrous tumor: a clinicopathologic correlation and review of literature. *Oman J Ophthalmol*. 2011;4:147–9.
- Krishnakumar S, Subramaniam N, Mohan ER, Mahesh L, Biswas J, Rao NA. Solitary fibrous tumor of the orbit: a clinicopathologic study of six cases with review of the literature. *Surv Ophthalmol*. 2003;48:544–54.
- Bernardini FP, de Conciliis C, Schneider S, Kersten RC, Kulwin DR. Solitary fibrous tumor of the orbit: Is it rare? Report of a case series and review of literature. *Ophthalmology*. 2003;110:1442–8.
- Tam ES, Chen EC, Nijhawan N, Harvey JT, Howarth D, Oestreich JH. Solitary fibrous tumor of the orbit: a case series. *Orbit*. 2008;27:426–31.
- Polito E, Tosi M, Toti P, Shurfeld K, Caporossi A. Orbital solitary fibrous tumor with aggressive behaviour: three cases and review of literature. *Graefes Arch Clin Exp Ophthalmol*. 2002;240:570–4.
- Chung HR, Tam K, Han AY, Obeidin F, Nakasaki M, Chhetri DK, St John MA, Kita AE. Solitary Fibrous Tumors of the Head and Neck: A Single-Institution Study of 52 Patients. *OTO Open*. 2022;6:2473974X221098709. <https://doi.org/10.1177/2473974X221098709>.
- Hong YT, Han S. Malignant Solitary Fibrous Tumor of the Nasal Cavity and Orbit: A Case Report. *Ear Nose Throat J*. 2022. <https://doi.org/10.1177/01455613221139406>. Epub ahead of print.
- Bahrami A, Lee S, Schaefer IM, Boland JM, Patton KT, Pounds S, Fletcher CD. TERT promoter mutations and prognosis in solitary fibrous tumor. *Mod Pathol*. 2016;29:1511–22.
- Demicco EG, Wani K, Ingram D, Wagner M, Maki RG, Rizzo A, Meeker A, Lazar AJ, Wang WL. TERT promoter mutations in solitary fibrous tumour. *Histopathology*. 2018;73:843–51.